Environmental Science Advances

ROYAL SOCIETY OF CHEMISTRY

PAPER

View Article Online
View Journal | View Issue

Cite this: *Environ. Sci.: Adv.*, 2023, **2**, 1210

Optical chemical sensors for soil analysis: possibilities and challenges of visualising NH_3 concentrations as well as pH and O_2 microscale heterogeneity†

Theresa Merl,[a] Yihuai Hu,[be] Johanna Pedersen,[b] Silvia E. Zieger,[a] Marie Louise Bornø,[c] Azeem Tariq,[cd] Sven Gjedde Sommer[b] and Klaus Koren *[a]

Agricultural nitrogen (N) application to soils is the main source of atmospheric ammonia (NH_3). Ammonia negatively impacts the environment on a large scale. However, emissions of NH_3 are affected by spatiotemporal heterogeneities of soil parameters on a microscale. Some key parameters controlling processes of the N cycle are soil oxygen (O_2) and pH. To better understand biogeochemical soil processes, NH_3 emissions and the interconnection of the ecospheres, we propose the application of optical chemical sensors (optodes) in and above soils. The use of optodes in soil science is in its infancy. In this laboratory-based study, we investigated the possibilities and challenges of using optodes in non-waterlogged soils with the extended application of a recently developed NH_3 optode along with pH and O_2 optodes in two different soils and with different fertilisers. Our intention is to help expand the use of optodes in soil science. Our results demonstrated the possibility to visualise reductions of NH_3 concentrations by 76% and 87% from the incorporation of sludge compared to the surface application of sludge. We showed from 2D measurements how soil pH and fertiliser composition correlate with NH_3 volatilisation. Our measurements demonstrated that pH optodes can have advantages over conventional methods when measuring pH in soils *in situ* but are challenged by the limited dynamic range (typically 3 pH units) compared to pH electrodes. Finally, we investigated the spatiotemporal dynamics of O_2 at different soil water contents and discuss potential challenges, which can lead to measuring artifacts.

Received 9th May 2023
Accepted 15th July 2023

DOI: 10.1039/d3va00127j

rsc.li/esadvances

Environmental significance

Soils are essential for food production and ecosystem services. The pedosphere, entailing soils, is at the intersection of the anthroposphere and all other ecospheres. Thus, soil processes impact element cycles and gas emissions. To ensure environmental health a holistic understanding of soil processes is required. This study shows the potential to use optical chemical sensors (optodes) within and above soils as tools to monitor soil and its connection to other spheres in 2D. This can provide quick valuable insights into soil–fertiliser interactions and chemical microenvironments regarding pH, O_2 and ammonia concentrations over time and space. Optodes can be used to obtain novel insights and to increase our understanding of the mutually affected relationship of ecospheres and anthropological activities.

1 Introduction

Soil is an important part of the pedosphere, which is directly connected to and impacted by the anthroposphere and the other ecospheres (atmosphere, biosphere, hydrosphere).[1] These interconnections have an impact on environmental quality, human health and sustainability.[2] In other words, soils facilitate life and feed the world population as they are the basis of healthy ecosystems and food production.[3] Soils are complex biological systems due to their high biogeochemical activity and spatiotemporal heterogeneities. Distinct physical, chemical, and biological soil properties create microsites within the soil matrix. These sites are involved in important soil processes, including both nutrient cycling and gas formation, as they are

[a]*Department of Biology, Aarhus University Centre for Water Technology, Aarhus University, Section for Microbiology, Ny Munkegade 114, 8000 Aarhus C, Denmark. E-mail: klaus.koren@bio.au.dk*

[b]*Department of Biological and Chemical Engineering, Aarhus University, Gustav Wieds Vej 10, 8000 Aarhus C, Denmark*

[c]*Department of Plant and Environmental Sciences, University of Copenhagen, Thorvaldsensvej 40, 1871 Frederiksberg, Denmark*

[d]*School of Environmental Sciences, University of Guelph, Ontario N1G2W1, Canada*

[e]*Department of Agroecology, Pioneer Centre Land-CRAFT, Aarhus University, C. F. Møllers Allé 4, 8000 Aarhus C, Denmark*

† Electronic supplementary information (ESI) available. See DOI: https://doi.org/10.1039/d3va00127j

highly influenced by soil heterogeneity.[4–7] Hence, the pedosphere is impacted by a mosaic of microenvironments and distinct chemical conditions on a small scale, which in turn impacts the other spheres on a large scale.

In agricultural soils, fertilisation and soil amendments affect the soil composition as well as soil properties. Different fertiliser management strategies may cause variations in soil pH, substrate availability, and O_2 within the soil matrix. Within the soil, the production and formation of ammonia (NH_3) are highly sensitive to changes in soil parameters such as soil moisture, pH, O_2, and different nitrogen (N) forms.[7,8] During the last century, N fertilisers were applied excessively to agricultural soils, thereby increasing the emissions of reactive N gases (*e.g.*, NH_3 and nitrous oxide (N_2O)).[9] NH_3 emissions from agriculture accounted for 96% of the European atmospheric NH_3 release, which contributes to the low efficiency of fertiliser uptake.[10] NH_3 emissions pose an environmental risk through N deposition, acidification, and eutrophication.[11] Furthermore, they contribute to the formation of atmospheric particulate matter ($PM_{2.5}$), which is associated with adverse human health effects as they can affect the lungs or other organs and can result in chronic respiratory illnesses.[12–14] Other health effects can stem from the direct impact of NH_3 and can include irritation to the eyes and throat and increased coughing, among others.[15] Thus, there is a great demand to mitigate NH_3 emissions.

To improve mitigation strategies, detailed insights into local processes and interactions of soil and fertilisers at the microscale are needed, as this could partially explain the great variabilities seen in NH_3 emission factors.[16] In addition, this can offer a new approach for expanding knowledge regarding the interconnections of the pedospehere (soils) with the atmosphere, biosphere and anthroposphere. Therefore, it is important to monitor concentrations of emitted NH_3 at soil/air and soil/fertiliser interfaces, and at the same time continuously measure spatiotemporal changes of important soil parameters in distinct microsites as these can provide a deeper understanding of NH_3 emission dynamics. To date, the general approach to studying soil processes and gas emissions relies on bulk measurements of soil compounds and gas concentrations. These bulk measurements fail to provide the spatial and temporal resolution, especially at the mentioned interfaces, needed for an in-depth understanding of these complex processes. Planar optical sensors, also termed optodes,[17,18] may provide a methodological platform for high-resolution spatiotemporal studies of soil processes.

Optodes are reversible optical sensors that enable monitoring of variations in analyte concentrations (*e.g.*, O_2, pH, NH_3, CO_2) for several days with imaging intervals ranging from seconds to hours. Thus, optodes offer non-invasive and *in situ* imaging of analytes at high spatial and temporal resolution and depending on the analyte it is possible to measure in different matrices such as soil air (O_2 and NH_3), soil water (O_2, NH_3, pH) or at reactive interfaces such as soil fertilisers (O_2, NH_3, pH). In short, optodes show a change in photoluminescence after interacting with an analyte.[19,20] They consist of an analyte-sensitive luminophore, which is immobilised within a polymer matrix and coated onto a support material, such as plastic foil. There are two possibilities for referenced readout, which are lifetime-based and ratiometric imaging.[18] Optodes show great promise for studying soil biochemistry as they visualise analyte changes in real-time and without sample pretreatment.

Some optodes, such as those used for pH and O_2, are well-established tools to study complex environments, in particular sediments and waterlogged soils.[21,22] However, only a few studies have applied optodes within non-waterlogged soils.[23–30] Most relevant soil processes, from an agricultural perspective, should be studied at lower water contents relevant for plant growth (40–90% of the water holding capacity (WHC)). Optodes for NH_3 (ref. 31–33) or NH_4^+ are mainly available for detecting low ppb_v concentrations and are rarely used in soils. Therefore, they are still not well characterised for gaseous NH_3 measurements in and above soils. Strömberg *et al.* proposed an NH_4^+ optode that could be used in soils, but despite a few studies, this optode has not been applied since then.[29,34,35] Recently, we developed a dedicated NH_3 optode working in a higher concentration range.[24] The new NH_3 optode is well suited for soil studies and it can be combined with other optodes to acquire complex spatiotemporal patterns in 2D.

This study aimed to identify the possibilities and challenges of using optodes in non-waterlogged soils and soils with different soil physicochemical characteristics. Another aim was to present these findings as a guide to aid the use of optodes in soil science, to avoid errors and to increase outcome opportunities. Therefore, optodes for NH_3, pH and O_2 were implemented in several laboratory soil experiments to assess their usability in different scenarios related to agricultural practices or natural events occurring within soils (Fig. 1). For this, dairy processing sludge (DPS) was chosen as an organic fertiliser. Dairy processing sludge is an emerging biobased fertiliser as it is an organic waste product rich in phosphorus (P) and N derived from the wastewater treatment of the dairy industry.[36] A reason for its use is the goal of more sustainability for food and agricultural systems.[37] The soils used were two loamy sandy soils typical of Danish agricultural soils and differed in their pH values. Additionally, pH optodes were tested to measure pH in non-waterlogged soils *in situ* and O_2 optodes to test the usability of such optodes at different soil water contents.

2 Materials and methods

2.1 Soil and dairy sludge

Two soils that differ in pH were used in the different optode studies (Table S1†). Soil 1, a sandy loam with a high organic matter content was collected from 0 to 20 cm depth from an experimental field site at Aarhus University, Foulum, Denmark (56° 30′ N, 9° 34′). The fresh soil was collected in late October 2020, passed through a 4 mm sieve, and stored in a cold room (4 °C) for two weeks until the implementation of the experiment. Soil 1 had a relatively low pH_{H_2O} of 5.6 (Table S1†). The second soil (Soil 2) was also a sandy loam with a naturally high content of calcium carbonate ($CaCO_3$) originating from the

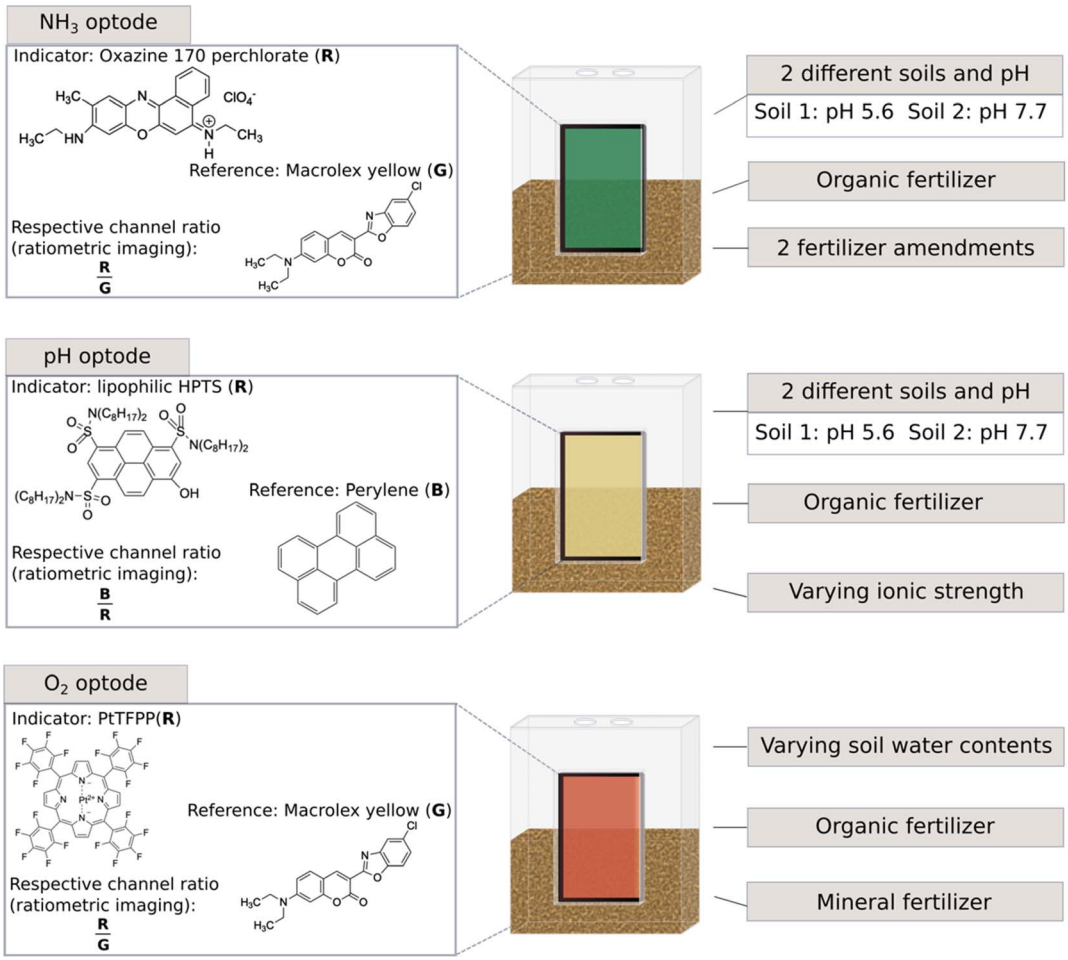

Fig. 1 Overview of the experimental set-up and utilised optodes as well as the various test scenarios, pH values were measured with a pH electrode.

surrounding moraine. This soil was collected in February 2021 from an agricultural field located in Tølløse, Zealand, Denmark (55° 37′ N, 11° 48′). After collection, the soil was passed through a 2 mm sieve and stored at 4 °C. This soil had a relatively high pH_{H2O} of 7.7 due to a high content of $CaCO_3$. The soil textures were characterised by AGROLAB Agrar/Umwelt (Sarstedt, Germany). Soil pH was measured in a 1 : 2.5 w/w soil/water ratio and with a microglass pH-electrode (type 6.0234.110, Metrohm, Herisau, Switzerland) connected to a pH meter (type 764, Knick, Berlin, Germany) with a temperature probe calibrated using standard pH buffers (Fluka Analytical). Further soil properties were analyzed and details can be found in the ESI.† The soil properties of Soil 1 and Soil 2 are listed in Table S1.†

DPS was obtained from a wastewater treatment plant of a dairy production factory in Videbæk, Denmark. The sludge had not been anaerobically digested before the addition of iron sulphide and separation with a decanting centrifuge. It was stored at −18 °C until three days prior to the start of the experiment. The chemical properties of DPS were measured by an accredited laboratory (Højvang laboratorier A/S, Denmark). Properties of the DPS are presented in Table S1.†

2.2 Experimental setup for NH_3, pH and O_2 measurements

A total of five studies were conducted to elucidate different aspects of implementing optodes in soil studies using different N fertilisers, optode combinations, soil types, and water contents. An overview of the different studies can be found in Table 1 and Fig. 1. For the experimental setup specially designed transparent plastic chambers with removable front walls and lids were used as measurement chambers ($L \times W \times H$: 60 × 39 × 100 mm) (Fig. 1 and S2†). Soil and fertilisers were incubated in the chambers, while optodes were fixed on an integrated glass window (50 × 50 mm) equipped on the front walls.

In all five studies (Table 1), the soils were packed into the chambers, achieving a soil bulk density of 1.3 g cm^{-3} resembling field soil bulk density. The soil packing method was adopted from Zhu *et al.*[38] and Nguyen *et al.*[39] In studies using Soil 1, the chambers were packed to 36 mm depth, and in studies with Soil 2, the chambers were packed to 38 mm depth, thus both the soil and the air above could be investigated through the optode window. The gravimetric soil water contents in studies 1–4 were kept at 35%, which corresponds to 80% and 93% of WHC for soils 1 and 2, respectively. This water content

Table 1 Overview of Studies 1–5 using ammonia (NH_3), pH and oxygen (O_2) optodes. The properties of the soils and DPS can be found in Table S1. DPS: dairy processing sludge

	Study 1	Study 2	Study 3	Study 4	Study 5
Soil	Soil 1	Soil 2	Soil 2	Soil 2	Soil 1
Soil $pH_{Electrode}$	5.6	7.7	7.7	7.7	5.6
Fertiliser type	DPS	DPS	DPS	DPS	Mineral fertiliser
Fertiliser application	Middle	Middle	Top and middle	Top and middle	Top
Duration	21 h/18 days	21 h	21 h	21 h	7 days
Gravimetric water content (%)	35	35	35	35	18, 25, 32
% of WHC	80	93	93	93	41, 57, 73
Optodes	NH_3, pH/O_2	pH	NH_3	NH_3	O_2

resembles moist non-waterlogged field soil. In all studies, the chambers were closed on top with a lid to ensure the soil water content remained constant.

In Studies 1–4, DPS was applied either in the middle of the soil (SM) or on top of the soil (ST) to monitor the differences in NH_3 emissions, pH, and in one case O_2 from these two treatments applied on the two different soils. The middle layer with DPS was a hotspot of a soil/sludge mixture where 5% and 4.4% (w/w) DPS were applied on a dry matter basis in Soils 1 and 2, respectively. The amount of sludge mixed into the layer was chosen to make up the air-porosity volume in the soil equal to the other layers. The amounts of soil, sludge, and water used for each layer can be found in the ESI.† In the ST treatments the same amount of DPS that was used to mix in the SM treatments was simply applied in a layer on top of the soil. Control chambers with no DPS amendments were included in all studies.

In order to investigate the difference in O_2 level at one constant gravimetric soil water content (35%) with DPS, one chamber was also equipped with an O_2 optode in Study 1 using Soil 1 and applying the sludge in the middle (SM). This was compared to Study 5. In Study 5, the use of O_2 optodes under different gravimetric soil water contents relevant for plant growth was investigated. Three different gravimetric water contents of 18%, 25% and 32% corresponding to 41%, 57% and 73% of WHC designated as low (*L*), medium (*M*), and high (*H*) water content, respectively, were included. This investigation was included to describe the more general use of optodes under agriculture-relevant water contents. The chambers were filled with Soil 1 and packed in the same way as described above, however, varying amounts of water were added. Instead of sludge, 750 mg of mineral fertiliser (calcium ammonium nitrate, CAN, Yara), equivalent to 101.25 mg NH_4–N, was distributed on the top. Furthermore, rain was simulated by adding equal amounts of water to each chamber to raise the water contents by 11%, which equals a 4.67 mm rain event. This altered the gravimetric soil water contents to 29% (Rain-L), 36% (Rain-M), and 43% (Rain-H), respectively.

2.3 Planar optode fabrication

Optodes for NH_3 were prepared as previously reported by Merl and Koren[24] and so were optodes for O_2 and pH.[24,40] A detailed description of the preparation steps can be found in the ESI.†

2.4 Imaging setup and measurement

In Studies 1 and 2, the imaging setup consisted of an SLR camera (EOS 1300D, Canon, Japan) combined with a macro-objective lens (Zoom lens EF-S18-55mm f/3.5-5.6 III, Canon, Japan), a yellow 455 nm long-pass filter (GG455 SCHOTT, 52 mm × 2 mm) with another plastic filter (#10 medium yellow; LEEfilters.com). The plastic filter was mounted in front of the long-pass filter to regulate the background fluorescence. A 405 nm UV LED (r–s components, Copenhagen, Denmark) paired with a short-pass filter (Hoya B-390 HFB 3925, UQG Optics, Cambridge, England) was used to excite the optodes. The LED, which functions as the flashlight, was controlled with a trigger box. This box is a USB-controlled LED driver unit (https://imaging.fish-n-chips.de/) and is operated using the Look@RGB (https://imaging.fish-n-chips.de/) software, which also enables the gathering of the sample images and simultaneously operates the SLR camera and LED.

In Studies 3, 4 and 5 the imaging setup differed in the SLR camera, which had the near-infrared filter removed (EOS 1300D, Canon, Japan), and a macro-objective lens (Macro 100 F2.8 D, Tokina, Japan), as well as an orange 530 nm long-pass filter (OG530 SCHOTT, 52 mm × 2 mm). Instead of a UV LED, a blue LED (470 nm) with a short-pass filter (Dichroic blue filter CDB-2511, UQG Optics, Cambridge, England) was used (Fig. S1†).

In ratiometric color imaging the different color channels of a camera are used to measure intensities and to generate ratios from the optode signals. That is because the camera's sensor uses the Bayer color filter to split the incident light into different colors: blue, green and red. As each optode comprises different analyte sensitive dyes (fluorescent indicator dyes), their characteristics and responses also vary. Therefore, different channels are used to calculate the ratios of the optodes as the dyes' luminescence dominate different channels in each optode. This is explained in more detail in a previous study.[41]

Calibrations were conducted prior to each experiment using the same setup as consecutively used in the respective experiment. Calibrations and data analysis for NH_3, O_2 and pH optodes were conducted as described by Merl and Koren[24] and previous studies.[41,42] In terms of the NH_3 optodes, it is important to emphasise that these were wet calibrations, meaning that different NH_3 concentrations (NH_3 (aq.) in mg L^{-1}) were reached through various additions of an ammonium chloride stock solution to a 0.5 M sodium hydroxide solution (pH > 12).

The high pH facilitated the equilibrium between NH_3 and NH_4^+ (pK_a 9.25) to be on the side of NH_3.[24] The measured ratios from the optodes were translated into NH_3 (g) ppm_v, which was calculated from the initial concentrations of NH_3 (aq.) in mg L^{-1} because of the wet calibration and with the Henry's law constant for NH_3 according to Hafner *et al.*[43] To assess the relative differences in NH_3 concentrations between treatments, the wet calibration (with recalculated NH_3 (g) concentrations in ppm_v) was applied to the gas phase measurements. This is the fastest and simplest procedure at this point.

In each study, images were taken every 10 minutes for the first hour, and then the interval was increased to an image every hour, then to an image every two hours, up to an image every three hours. Images were acquired for a total of 21 hours for all studies except the studies using O_2 optodes, in these long-term imaging was conducted for 7 days and up to 18 days.

3 Results and discussion

In terms of agricultural practices, the main aim is to adjust the fertiliser management in a way that most of the applied N is utilised by the crops and to mitigate N loss (*e.g.*, *via* NH_3 or N_2O emissions). Hence, the NH_3 optodes' applicability as a screening method was assessed by investigating NH_3 concentrations resulting from varying fertiliser amendments in the airphase above the soil. Due to the interdependencies of NH_3 emissions with soil O_2 and pH, we also tested optodes for these analytes in similar settings as those chosen for the NH_3 optodes with the only difference of using those optodes inside the soil. These settings comprised non-waterlogged soils and the same organic fertiliser (DPS). Due to the higher dry matter content of DPS compared to manure, it was possible to keep the soil non-waterlogged while using an organic fertiliser. Below, we show the findings of the usability and challenges of optodes in agricultural settings and non-waterlogged soils.

3.1 Ammonia optode performance in different soils and DPS application strategies

The possibility to monitor differences in NH_3 concentrations with optodes was tested from dairy sludge (DPS) applied on top of the soil (ST) and from DPS incorporated into the middle of the soil (SM). This was performed in Studies 3 and 4 using Soil 2 with pH 7.7 and adjusting the gravimetric soil water content to 35%. Examples of images and the concentration change over time are shown in Fig. 2 for the NH_3 optode from Study 3. Regions of interest (ROIs) were chosen to represent the headspace above the soil and to illustrate the differences in NH_3 dynamics. Higher NH_3 concentrations above the soil resulted from the ST treatment compared to the SM treatment. The results from Study 4 show the same pattern and can be found in the ESI (Fig. S5†). In both treatments, a sudden spike in NH_3 concentration can be seen immediately after sludge application. The comparison of the maximum NH_3 concentrations from the initial timepoints resulted in four times higher NH_3 in the ST treatment than in the SM treatment in Study 3 (Fig. 2B) and around seven times higher NH_3 in Study 4 (Fig. S5†). Differences in the NH_3 concentrations between Study 3 and 4 could be due to a slight difference in the thawing and handling of the DPS in the experimental setup. In Study 4 the DPS was not completely thawed at the time of application, thus, infiltration differences of the sludge could have occurred as it is assumed that the more liquid (completely thawed) the fertiliser the faster the infiltration of such fertilisers, and this with the lower temperature of the sludge in the beginning can result in lower NH_3 concentrations. The incorporation of sludge (SM) led to reductions of NH_3 concentrations by 76% and 87% (calculated from ROIs at the first time points from ST and SM) in Studies 3 and 4, respectively, compared to the surface application of sludge (ST). These values of reduction in NH_3 concentration are within the range reported by Monaco *et al.* for a laboratory scale experiment investigating the NH_3 reduction from the incorporation of pig slurry compared to surface-applied slurry, which yielded an 81.7% reduction in NH_3.[44] In field studies with the same objective, reductions in NH_3 of 40–60% (ref. 45) and 80% (ref. 46) were reported. Additionally, the immediate high NH_3 concentrations resulting from the surface application of fertiliser were also observed in laboratory scale experiments[44] and in field studies.[45] Upon the immediate NH_3 release, a decline in NH_3 concentrations followed for about two hours. Similar concentration profiles over time were also seen in previous studies.[24,44] The decline in NH_3 could be because the chambers were not completely air-tight. Another reason for the decline could be the pH, as an increase in surface pH of the soil/sludge mixture probably occurred due to emission of CO_2 immediately after sludge application followed by a gradual decline in pH, hence also in NH_3, due to the buffering capacity of the soil. Lower NH_3 concentrations in the treatments with sludge applied in the middle are observed due to the soil creating a barrier, which induces a complete air-side resistance.[47]

These NH_3 concentrations are not to be considered absolute values but rather as a method to assess relative differences between treatments. There are two reasons for that. Firstly, we observed that the wet calibration is not directly applicable to the gas phase concentrations due to changes in humidities and because the newly developed NH_3 optodes are humidity dependent (*e.g.*, the concentration measurements vary with humidity). The humidity dependency of the NH_3 optodes as well as the need to calibrate in the gas phase are not yet fully explored and need further investigations. Secondly, the chambers were kept closed while imaging NH_3 in the attempt to have well-defined soil system boundaries and thus eliminate the need to account for fluxes of energy and matter.[3] However, the emission of NH_3 is mainly restricted by the air-side resistance,[47] therefore, chambers without a continuous air-flow will restrain the NH_3 emission due to an increased laminar film boundary and consequently an increased gas-phase NH_3 concentration is obtained compared to natural field conditions.[48]

The impact soil pH has on NH_3 concentrations can also be assessed using optodes as seen in Fig. 3, which is supported by the false color images of the NH_3 (Fig. S8†) and pH (Fig. S7†) optodes. In three studies sludge with a pH of 7.8 was applied into the middle of soils with different pH values. In Study 1, soil with a pH of 5.6 (Soil 1) and in Studies 3 and 4 soil with a pH of

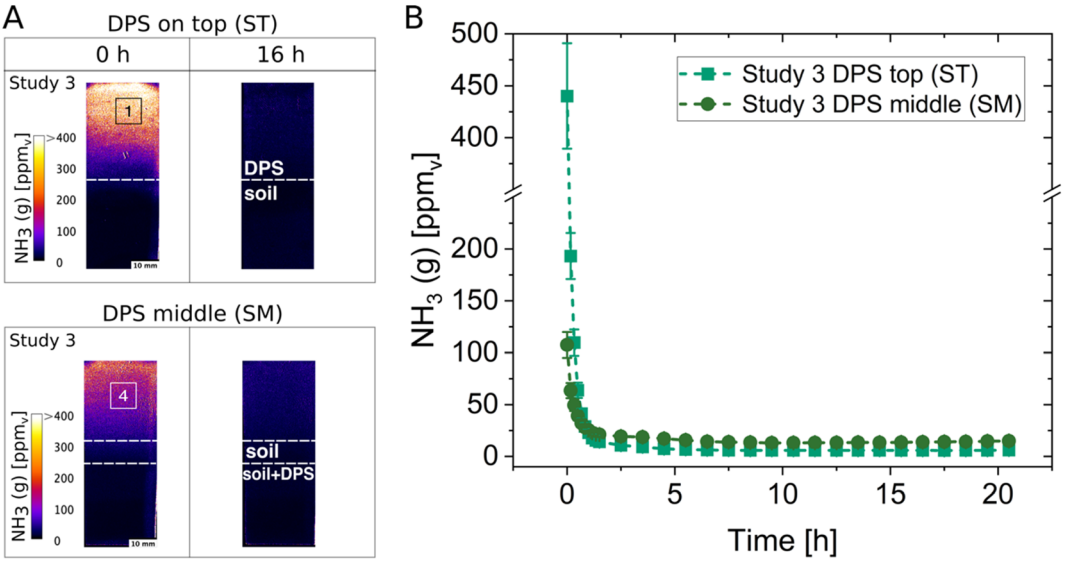

Fig. 2 (A) False color images showing the NH_3 concentrations of Study 3 with the treatment organic fertiliser (DPS) on top (ST) and in the middle (SM). These false color images are examples from the start (0 h) and from a timepoint at 16 h. The dotted lines indicate where the soil and mixture of soil and slurry interphase start. (B) NH_3 concentrations from the regions of interest (ROIs) 1 and 4 as can be seen in (A) over a period of 20 h. All error bars show the technical standard deviation (variability within the optodes).

7.7 (Soil 2) was used. The pH-dependent equilibrium of NH_3 and NH_4^+ causes NH_3–N to be mostly present as NH_4^+ (100%) at pH 6, whereas an increase to pH 8 results in a shift where both forms NH_4^+ (90%) and NH_3 (10%) are present, all else being equal (Fig. 3A). This shift in pH resulted in two and six times higher NH_3 concentrations above the soil in Study 3 and 4, respectively, compared to Study 1 (Fig. 3B). The low pH soil (Soil 1) must have buffered the pH of the sludge, which was higher than the soil, and this resulted in lower NH_3 concentrations compared to the amendment of the same sludge in Soil 2. The difference in the pH of the amended sludge in Soil 1 and Soil 2 as well as the heterogeneity of the pH changes due to the sludge can be seen in Fig. S7† as a result of the same amendments as discussed in Fig. 3. These results emphasise the importance of the chemical microenvironment of the soil in NH_3 emissions. This and a prior study[24] show that it can be advantageous to employ optodes for NH_3 and pH simultaneously as they can depict these interdependent and important processes further and on a high spatiotemporal scale.

3.2 Using optodes to measure spatiotemporal variations in soil pH

Soil pH is a key parameter in soil fertility, as it controls redox reactions, nutrient and toxin bioavailability and affects important biological processes.[49,50] This makes soil pH a parameter of general importance, and *in situ* and constant monitoring will contribute to a better understanding of the complexity of soils.

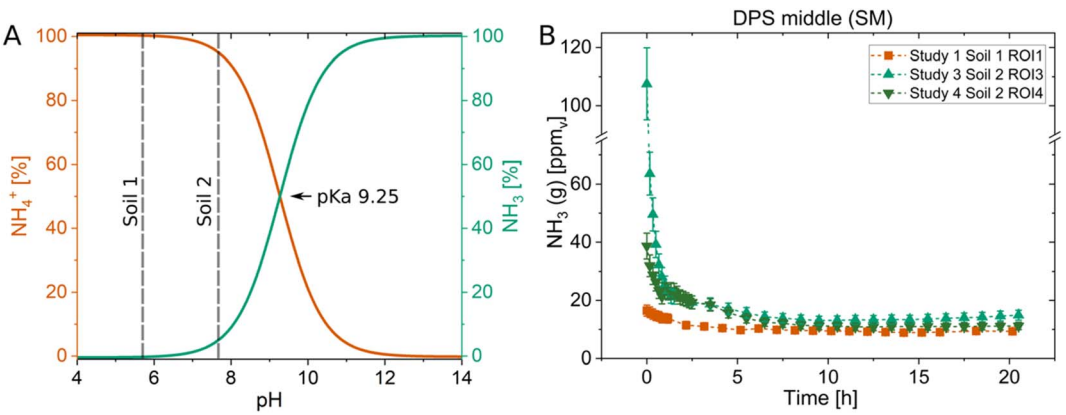

Fig. 3 (A) The pH-dependent equilibrium between ammonium (NH_4^+) and ammonia (NH_3) where the dotted lines show the pH the two soil samples (Soil 1 and Soil 2) had. (B) NH_3 concentrations of the regions of interest (ROIs) taken from the air interphase above the soil from each study (Study 1, 3 and 4) over a period of 20 hours to show the NH_3 emission from Soil 1 and Soil 2 with the treatment (SM) organic fertiliser (dairy sludge) amended in the middle. All error bars show the technical standard deviation (variability within the optodes).

Traditionally, soil pH is assessed with conventional laboratory pH measuring methods utilising potentiometric pH electrodes (in aqueous or mild saline extracts).[49] While pH glass electrodes are fast and cover a wide pH range, they can only measure bulk pH in samples where the soil-to-solution ratio is changed to unnatural ratios.[51] Therefore, *in situ* pH measurements at the soil's native gravimetric soil water content or spatially resolved measurements are not possible. This way, hotspots of pH changes cannot be determined in a complex system such as soil. Optical sensors for pH, on the other hand, can be used *in situ*, without the need for sample extraction, and can therefore unravel the spatial and temporal pH heterogeneities of soils.[49] However, both methods have their limitations regarding precise pH measurements, which come from different non-thermodynamic assumptions inherent in their modes of operation.[52] Due to that, an important differentiation between optical pH sensing and potentiometric pH measurements needs to be considered, which is that optical pH sensors base pH measurements on the concentration of a pH-sensitive dye, whereas pH is measured as the activity of hydrogen (H^+) ions in the potentiometric approach.[51,52] The latter is also the definition of pH in solution but soils cannot always be in solution if the pH needs to be assessed in a non-waterlogged state. Soil ionic strength is another example that contributes to biased pH measurements and is a soil parameter of great importance known to have large variances.[53] Even though optical pH sensors also show cross-sensitivity to ionic strength, the effect can be rather small.[54] A minimal effect of ionic strength on the response can be achieved, especially by using non-charged pH-sensitive dyes[54] as the one used in the pH optodes described in this study. The diminished impact different ionic strengths have on the used pH optode is illustrated in Fig. S6† and shows the slight differences in ratios at the same pH values but with three different ionic strengths (IS 0.10, 0.38 and 1.00 M).

Despite the advantages optical pH sensors bring to soil analysis they have not been used extensively in non-waterlogged soils so far. To expand beyond current approaches, we wanted to demonstrate the applicability of pH optodes in soils with lower soil water contents than in completely waterlogged soils, as waterlogged soils are not appropriate to study most relevant soil processes. We kept the gravimetric water content of both soils at 35%, corresponding to 93% of water holding capacity, which is a relevant water content when considering the agricultural production. Here we show that pH optodes are indeed suited for soils with lower soil water content when considering some of the optical sensor's limitations. Fig. 4A depicts a pH optode calibration curve with the dynamic range being between pH 5.5 and pH 8.5 and where the two soil samples' pH values are located within that range. While potentiometric pH sensors cover a wide pH range, optical pH sensors only cover a range of maximally 3 pH units, but their accuracy is superior to that of the potentiometric pH sensor within the sensitive range.[51] The highest sensitivity of a pH-sensitive indicator dye is reached at pH = pK_a, and the limitation of the pH range is attributed to pH = $pK_a \pm 1.5$. pH measurements with optical sensors (optodes) work well in a non-waterlogged soil sample if the soil pH is well within the range of the optode as seen in Fig. 4A for Soil 2, but

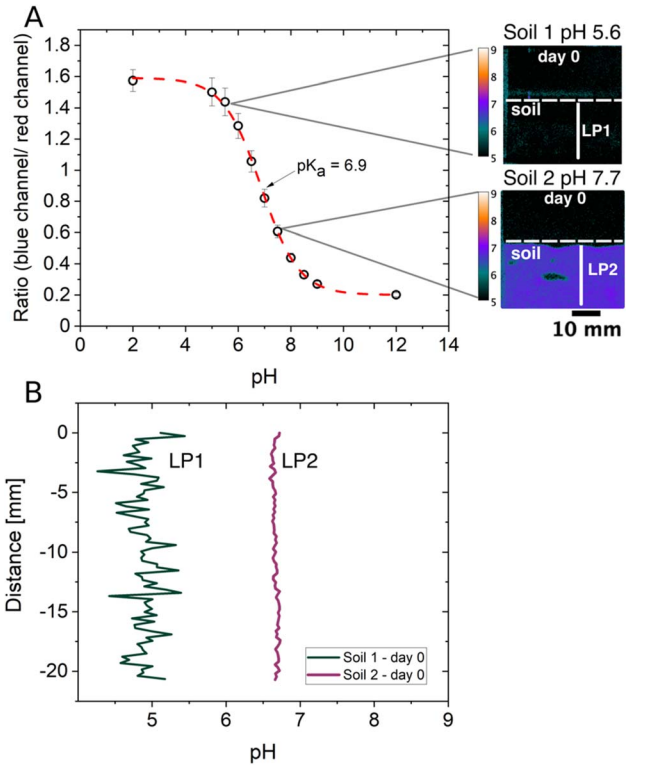

Fig. 4 (A) pH calibration curve showing the pK_a of the respective pH optode and the dynamic range. Error bars depict the minima and maxima of the chosen regions of interest for each calibration step. (B) Line profiles resulting from Study 1 using Soil 1 ($pH_{Electrode}$ 5.6), LP1, and Study 2 using Soil 2 ($pH_{Electrode}$ 7.7), LP2, where no sludge was added in either of the shown images.

not so well if a soil sample is just at the edge of that range as seen for Soil 1 (Fig. 4A). The polymer that is used in the pH optode could be the reason pH measurements are possible in non-waterlogged soil samples. The optical sensor in this study was prepared with a hydrogel (Hydromed D4), which is known to have the characteristic of 50% water absorption.[55] The polymer absorbs water present in the sample and swells, which is an advantage in facilitating proton exchange and detection even at relatively low soil water contents.

As soon as the soil's pH value is outside of the dynamic range the false color image in Fig. 4A and the line profile 1 (LP1) from Soil 1 in Fig. 4B show that it is not possible to achieve proper pH measurements. LP1 shows a rather noisy signal as the detection limit of the pH optode is reached while LP2 from Soil 2 results in much better signal qualities as it lies well within the dynamic range. This shows that it is important to consider the optical sensor's working range and to investigate the soil system's characteristics in advance. Despite the proposed considerations that need to be taken into account before using optical sensors for soil pH analysis, we still think it is a good approach for *in situ* measurements at lower soil water content. Nielsen *et al.* found that the conventional laboratory pH measurements for soils with suspension samples continuously overestimated the pH compared to *in situ* bulk pH measurements directly in the field.[56] The *in situ* pH values were 0.5–0.8 pH units lower than

the pH values measured with the extraction method in the laboratory. A similar trend was observed in one of our recent studies where *in situ* bulk measurements with small optode sensor spots were performed.[57] This is expected as the dilution of the soil with water results in lowering the electrolyte concentration, which leads to less protons to be exchanged into the soil solution, if the soil bares a net negative charge at its native pH.[57] The soils used in this study were also measured in a soil water suspension (soil : deionized water 1 : 2.5 w/w), resulting in a soil pH of 5.6 (Soil 1) and a soil pH of 7.7 (Soil 2). The *in situ* measurements with the pH optodes, however, revealed a soil pH of around pH 5 for Soil 1 and a soil pH of pH 6.6 for Soil 2. This reveals lower pH measurements with the pH optodes here too, with a difference of 0.6 units for Soil 1 and 1.1 units for Soil 2. Possible reasons for the higher pH values measured with the standard laboratory method could be the different modes of operation,[52] the release of buffering ions from soil biota due to drying, extraction, and rewetting of soil samples[56] or the change in electrolyte concentration due to dilution of the soil with water. Hence, it should become more common practice to choose *in situ* pH measurements over the standard method to avoid sample handling artifacts.

3.3 Oxygen optodes in non-waterlogged soils

In situ measurements of soil O_2 contents with optical sensors have been investigated in a number of studies, especially in combination with amendments of organic fertilisers.[23,27,28] That is because the availability and spatial distribution of O_2 have immense impacts on C and N cycling as well as greenhouse gas emissions. However, most of these studies were conducted in soils with high soil water content, partly due to the addition of liquid manure as an organic fertiliser. In this study, we investigated the usability of O_2 optodes related to the difference in O_2 distribution in soils with different gravimetric soil water contents and added a mineral and an organic fertiliser (Fig. 5). It can be seen in Fig. 5 that oxic conditions dominated for the first seven days after a mineral fertiliser was applied to the top of the soil. In contrast, O_2 depletion zones immediately formed when an organic fertiliser was applied and mixed within the middle area of the soil, which is due to the more easily biodegradable organic C in the sludge stimulating greater microbial activity. The O_2 depletion zones expanded to the surrounding soil for the next days. On day 4 a small zone of O_2 increase could be seen within the sludge and soil band (Fig. 5, bottom). It looks like excess O_2 diffusion or O_2 production occurred. The latter, however, is very unlikely as there were no plants and therefore no plant roots were involved in this sample to explain such a rise in O_2 levels. More likely though is the detachment of soil from the optode and O_2 influx from the headspace to that area. This highlights how important it is that the sample is in good contact with the optode to not misinterpret measured artifacts. The risk for artifacts like these might be minimized through packing the soil or the sample properly. Nevertheless, such artifacts can never be fully excluded as the sample's composition could induce deformation or detachment from the sensor even after days of measuring. Therefore, it is important to continuously analyze the data and the experiment to either try to establish contact again if the experiment's scope allows or to terminate the experiment.

Another challenge that is presented here is the measurement of O_2 dynamics at different soil water contents. This can be seen in Fig. 5 in the treatment with the mineral fertiliser on top where the soil with gravimetric water contents from 18 to 32% is fully oxygenated. And only after increasing the soil water content to 36% and 43%, an anoxic zone within the soil is formed. This supports the fact that O_2 diffusion becomes limited as soon as the soil becomes more waterlogged. It also shows that air filled pore spaces filled up with water after irrigation, which supports the increase of the anoxic area. Another interesting observation is that the oxygen depletion zones start from the bottom on day 7.2 (Fig. 5) instead of from the top, which could be because it is a sandy loam soil and not a clay soil. The formation of anoxic zones in the bottom first instead of the top layer could also be due to preferential flows along the boundaries of the soil and the inner chamber walls. Additionally, O_2 diffusion happens from the top, leading to the O_2 taking longer to reach the bottom as it is being used up on the way. This issue is increased if the water accumulates at the bottom. Even though O_2 optodes show a fully oxygenated soil under certain soil water contents, it does not necessarily mean that the oxygen concentrations shown with this measurement method depict the whole complexity of the O_2 dynamics. Anoxic zones can be present within soil particles, as shown by Revsbech *et al.*[58] by using a Clark-type microsensor for O_2 within small soil particles. Even though optodes offer a high-resolution measurement together with the possibility of imaging

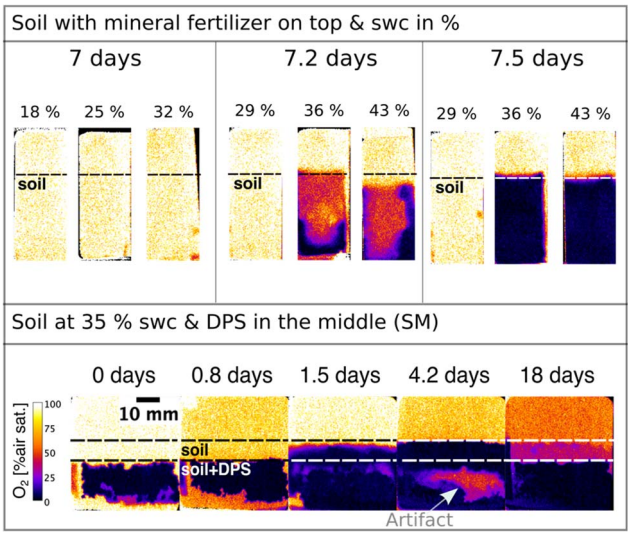

Fig. 5 False color images of the oxygen (O_2) concentration from Study 5 upon addition of the synthetic fertiliser and the images were taken for 7 days at the three different soil water contents (swc) (18%, 25% and 32%) showing one of the two replicates per soil water content. The image at the timepoint 7.2 days was taken after 11.5 mL of water was added to simulate a rain event. This heightened the soil water contents to 29%, 36%, and 43%. Only 8 hours (7.5 days) later the third panel shows the chambers with soil water contents of 36% and 43% with anoxic zones. Additionally, the false color images of the O_2 concentration of Study 1 are shown. In this study a soil water content of 35% was maintained and an organic fertiliser was applied in the middle part of the packed soil. Imaging was conducted for 18 days.

heterogeneities, it also showcases the limitations of this method as it is a bulk measurement compared to even higher resolution methods such as microsensors. This together with the need for contact between the sample and optode are not necessarily shortcomings of O_2 optodes in soils but rather challenges that need to be considered when designing the study.

4 Conclusion

Overall, the studies show that optodes can be a valuable additional tool in the soil analysis toolbox. They can be used to get a more holistic overview of fertiliser impacts due to their abilities and the possibility to combine them in the same system if their limitations are taken into consideration.

Our results demonstrated the ability to visualise the relative differences in NH_3 concentrations resulting from varying fertiliser amendments and from different soil pH values. On a large scale, such changes in concentration could have a big effect. Hence, the advantage of such short-term experiments can be to offer a preliminary assessment of the impact of new fertilisers, application techniques and soil–fertiliser interactions, and what that could mean on a bigger scale and for more than one area of interest (soil and airphase) measured at the same time. Therefore, a fast information transfer can be offered due to the reduction in laborious and costly field experiments for soil and fertiliser analysis with high spatiotemporal resolution. The interpretations of the NH_3 optode results, though, still need to be considered relative values due to a possible humidity dependency to allow more accurate gas phase measurements. Our measurements showed that pH optodes are a great alternative to conventional methods when it comes to measuring pH in soils *in situ*. Additionally, it is important to be aware of the diminished dynamic range pH optodes operate in compared to potentiometric sensors. In regard to O_2 optodes, we showed that it is not always feasible to measure spatiotemporal dynamics of O_2 if soil water contents are too low. The settings of the biological system need to be considered first regarding soil water content, organic matter, and processes that might occur. Another aspect regarding all optodes is their temperature dependency, which is predictable and can be corrected for[59] or circumvented by keeping the temperature stable throughout laboratory-based experiments. In addition, this approach entails a relatively cheap setup[41] as well as commercially available compounds for most of the optodes. This offers easy accessibility to use this approach as also low time commitment is sufficient to use the setup and to acquire the skillset of the optode preparation.[60]

Showcasing the possibilities as well as the challenges of optodes in soil systems could aid in bridging the gap among fields. This will help broadening our understanding of complex soil processes and how these are linked to emissions from the agricultural sector, environmental quality and human wellbeing by adding missing links of spatiotemporal variations within the soil and at the soil/air interphase.

Conflicts of interest

There are no conflicts of interest to declare.

Acknowledgements

This study was supported by research grants from the Poul Due Jensen Foundation (KK), a Sapere Aude grant from the Independent Research Fund Denmark (IRFD): DFF-8048-00057B (KK), a Green Development and Demonstration Program (GUDP) from the Ministry of Food, Agriculture and Fisheries of Denmark (journal nr.: 34009-21-1829) (JP), the European Union's Horizon 2020 Marie Skłodowska-Curie Actions (MSCA) Innovative Training Networks (ITN) (No. 814258) (YH), and the project INTERACT funded by the Novo Nordisk Foundation (grant no.: NNF19SA0059360) (MLB). The authors want to thank Lars Borregaard Pedersen and Mette L. G. Nikolajsen for the excellent technical support.

References

1 R. Lal, R. H. Mohtar, A. T. Assi, R. Ray, H. Baybil and M. Jahn, *Curr. Sustainable Energy Rep.*, 2017, **4**, 117–129.
2 Y. Chang, G. Li, Y. Yao, L. Zhang and C. Yu, *Energies*, 2016, **9**, 1–17.
3 D. G. Strawn, H. L. Bohn and G. A. O'Connor, *Soil Chemistry*, John Wiley & Sons, Ltd, The Atrium, Southern Gate, Chichester, West Sussex, PO19 8SQ, UK, 4th edn, 2015.
4 N. Nunan, H. Schmidt and X. Raynaud, *Philos. Trans. R. Soc., B*, 2020, **375**, 20190249.
5 K. A. Smith, *Eurasian J. Soil Sci.*, 2017, **68**, 137–155.
6 J. L. Wilmoth, *Sustainability*, 2021, **13**(18), 10084.
7 K. C. Cameron, H. J. Di and J. L. Moir, *Ann. Appl. Biol.*, 2013, **162**, 145–173.
8 D. A. Turner, R. E. Edis, D. Chen, J. R. Freney and O. T. Denmead, *Nutr. Cycling Agroecosyst.*, 2012, **93**, 113–126.
9 X. Zhang, E. A. Davidson, D. L. Mauzerall, T. D. Searchinger, P. Dumas and Y. Shen, *Nature*, 2015, **528**, 51–59.
10 E. Giannakis, J. Kushta, A. Bruggeman and J. Lelieveld, *Environ. Sci. Eur.*, 2019, **31**, 93.
11 S. G. Sommer, J. K. Schjoerring and O. T. Denmead, *Adv. Agron.*, 2001, **82**, 557–622.
12 V. P. Aneja, W. H. Schlesinger and J. W. Erisman, *Environ. Sci. Technol.*, 2009, **43**, 4234–4240.
13 J. T. Walker, W. P. Robarge, A. Shendrikar and H. Kimball, *Environ. Pollut.*, 2006, **139**, 258–271.
14 D. Giannadaki, E. Giannakis, A. Pozzer and J. Lelieveld, *Sci. Total Environ.*, 2018, **622–623**, 1304–1316.
15 K. E. Wyer, D. B. Kelleghan, V. Blanes-Vidal, G. Schauberger and T. P. Curran, *J. Environ. Manage.*, 2022, **323**, 116285.
16 S. D. Hafner, A. Pacholski, S. Bittman, W. Burchill, W. Bussink, M. Chantigny, M. Carozzi, S. Génermont, C. Häni, M. N. Hansen, J. Huijsmans, D. Hunt, T. Kupper, G. Lanigan, B. Loubet, T. Misselbrook, J. J. Meisinger, A. Neftel, T. Nyord, S. V. Pedersen, J. Sintermann, R. B. Thompson, B. Vermeulen, A. V. Vestergaard, P. Voylokov, J. R. Williams and S. G. Sommer, *Agric. For. Meteorol.*, 2018, **258**, 66–79.
17 M. Schäferling, *Angew. Chem., Int. Ed.*, 2012, **51**, 3532–3554.
18 O. S. Wolfbeis, *J. Mater. Chem.*, 2005, **15**, 2657–2669.

19 J. Santner, M. Larsen, A. Kreuzeder and R. N. Glud, *Anal. Chim. Acta*, 2015, **878**, 9–42.
20 K. Koren and S. E. Zieger, *ACS Sens.*, 2021, **6**, 1671–1680.
21 C. Li, S. Ding, L. Yang, Q. Zhu, M. Chen, D. C. W. Tsang, G. Cai, C. Feng, Y. Wang and C. Zhang, *Earth Sci. Rev.*, 2019, **197**, 102916.
22 K. Koren and M. Kühl, in *Quenched-phosphorescence Detection of Molecular Oxygen: Applications in Life Sciences*, ed. D. B. Papkovsky and R. I. Dmitriev, Royal Society of Chemistry, 2018, 1, pp. 145–174.
23 K. Zhu, X. Ye, H. Ran, P. Zhang and G. Wang, *Soil Biol. Biochem.*, 2022, **166**, 108564, DOI: **10.1016/j.soilbio.2022.108564**.
24 T. Merl and K. Koren, *Environ. Int.*, 2020, **144**, 106080.
25 N. Rudolph-Mohr, C. Tötzke, N. Kardjilov and S. E. Oswald, *Zeitschrift fur Pflanzenernahrung und Bodenkd*, 2017, **180**, 336–346.
26 W. Christel, K. Zhu, C. Hoefer, A. Kreuzeder, J. Santner, S. Bruun, J. Magid and L. S. Jensen, *Sci. Total Environ.*, 2016, **554–555**, 119–129.
27 K. Zhu, S. Bruun, M. Larsen, R. N. Glud and L. S. Jensen, *J. Environ. Qual.*, 2014, **43**, 1809–1812.
28 Q. Van Nguyen, L. S. Jensen, R. Bol, D. Wu, J. M. Triolo, A. H. Vazifehkhoran and S. Bruun, *J. Environ. Qual.*, 2017, **46**, 1114–1122.
29 S. Delin and N. Strömberg, *Eur. J. Soil Sci.*, 2011, **62**, 295–304.
30 N. Strömberg, J. Engelbrektsson and S. Delin, *Sens. Actuators, B*, 2009, **140**, 418–425.
31 K. Waich, S. Borisov, T. Mayr and I. Klimant, *Sens. Actuators, B*, 2009, **139**, 132–138.
32 T. Abel, B. Ungerböck, I. Klimant and T. Mayr, *Chem. Cent. J.*, 2012, **6**, 1–9.
33 B. J. Müller, N. Steinmann, S. M. Borisov and I. Klimant, *Sens. Actuators, B*, 2018, **255**, 1897–1901.
34 N. Strömberg, *Environ. Sci. Technol.*, 2008, **42**, 1630–1637.
35 N. Strömberg and S. Hulth, *Anal. Chim. Acta*, 2001, **443**, 215–225.
36 W. Shi, M. G. Healy, S. M. Ashekuzzaman, K. Daly, J. J. Leahy and O. Fenton, *J. Clean. Prod.*, 2021, **314**, 128035.
37 European Commission, *Farm to Fork Strategy: for a Fair, Healthy and Environmentally-Friendly Food System*, 2020.
38 K. Zhu, S. Bruun, M. Larsen, R. N. Glud and L. S. Jensen, *Soil Biol. Biochem.*, 2015, **84**, 96–106.
39 Q. Van Nguyen, D. Wu, X. Kong, R. Bol, S. O. Petersen, L. S. Jensen, S. Liu, N. Brüggemann, R. N. Glud, M. Larsen and S. Bruun, *Soil Biol. Biochem.*, 2017, **114**, 200–209.
40 K. E. Brodersen, K. Koren, M. Moßhammer, P. J. Ralph, M. Kühl and J. Santner, *Environ. Sci. Technol.*, 2017, **51**, 14155–14163.
41 M. Larsen, S. M. Borisov, B. Grunwald, I. Klimant and R. N. Glud, *Limnol. Oceanogr.: Methods*, 2011, **9**, 348–360.
42 K. E. Brodersen, K. Koren, M. Moßhammer, P. J. Ralph, M. Kühl and J. Santner, *Environ. Sci. Technol.*, 2017, **51**, 14155–14163.
43 S. D. Hafner, F. Montes and C. Alan Rotz, *Atmos. Environ.*, 2013, **66**, 63–71.
44 S. Monaco, D. Sacco, S. Pelissetti, E. Dinuccio, P. Balsari, M. Rostami and C. Grignani, *J. Agric. Sci.*, 2012, **150**, 65–73.
45 K. A. Smith, D. R. Jackson, T. H. Misselbrook, B. F. Pain and R. A. Johnson, *J. Agric. Eng. Res.*, 2000, **77**, 277–287.
46 S. G. Sommer, E. Friis, A. Bach and J. K. Schjørring, *J. Environ. Qual.*, 1997, **26**, 1153–1160.
47 N. Hudson and G. A. Ayoko, *Bioresour. Technol.*, 2008, **99**, 3982–3992.
48 B. Eklund, *J. Air Waste Manage. Assoc.*, 1992, **42**, 1583–1591.
49 M. Nadporozhskaya, N. Kovsh and R. Paolesse, *Chemosensors*, 2022, **10**, 35.
50 W. Buss, J. G. Shepherd, K. V. Heal and O. Mašek, *Geoderma*, 2018, **331**, 50–52.
51 A. Steinegger, O. S. Wolfbeis and S. M. Borisov, *Chem. Rev.*, 2020, **120**(22), 12357–12489.
52 J. Janata, *Anal. Chem.*, 1987, **59**, 1351–1356.
53 G. W. Thomas, in *Methods of Soil Analysis*, John Wiley & Sons, Ltd, 1996, pp. 475–490.
54 S. M. Borisov, D. L. Herrod and I. Klimant, *Sens. Actuators, B*, 2009, **139**, 52–58.
55 Hydromed, **http://www.advbiomaterials.com/products/hydrophilic/HydroMed.pdf**.
56 K. E. Nielsen, A. Irizar, L. P. Nielsen, S. M. Kristiansen, C. Damgaard, M. Holmstrup, A. R. Petersen and M. Strandberg, *Soil Biol. Biochem.*, 2017, **115**, 63–65.
57 T. Merl, M. R. Rasmussen, L. R. Koch, J. V. Søndergaard, F. F. Bust and K. Koren, *Soil Biol. Biochem.*, 2022, **175**, 4–6.
58 A. J. Sexstone, N. P. Revsbech, T. B. Parkin and J. M. Tiedje, *Soil Sci. Soc. Am. J.*, 1985, **49**(3), 645–651.
59 E. Fritzsche, C. Staudinger, J. P. Fischer, R. Thar, H. W. Jannasch, J. N. Plant, M. Blum, G. Massion, H. Thomas, J. Hoech, K. S. Johnson, S. M. Borisov and I. Klimant, *Mar. Chem.*, 2018, **207**, 63–76.
60 M. Moßhammer, V. V. Scholz, G. Holst, M. Kühl and K. Koren, *J. Vis. Exp.*, 2019, 1–10.